


Imaging Characteristics and Clinical Outcomes of Biphenotypic Sinonasal Sarcoma

Amar Miglani, MD ; Devyani Lal, MD; Steven M. Weindling, MD; Christopher P. Wood, MD;
Joseph M. Hoxworth, MD

Objectives: Biphenotypic sinonasal sarcoma (BSS) is a new, rare tumor characterized by concomitant neural and myogenic differentiation. The aim of this study is to describe the imaging characteristics and clinical outcomes of this neoplasm.

Methods: A retrospective review of BSS patients surgically treated within a tertiary academic health care system was performed. Imaging characteristics and clinical outcomes were reviewed.

Results: Five patients underwent surgical resection of BSS tumors. Negative surgical margins were achieved in four (80%) patients. There were no deaths but two (40%) patients developed local recurrences during the postoperative follow-up period (median follow-up 31.4 months). Review of imaging characteristics revealed a median tumor size of 3.8 cm in greatest dimension. All tumors were unilateral and centered within the nasoethmoidal region. In all cases, the tumors extended to the nasal septum, lamina papyracea, and anterior skull base with variable degrees of erosion through these structures. On CT, involved bony structures demonstrated mixed lytic and sclerotic pattern, with definitive hyperostotic bone identified in four (80%) cases. On MRI, tumors were isointense-to-mixed iso/hypointense on both T1- and T2-weighted sequences with one tumor demonstrating mixed T2 hyperintensity. All cases demonstrated gadolinium contrast enhancement.

Conclusions: BSS is a locally aggressive tumor with a low risk of regional or distant metastases but has a significant rate of recurrence even with adequate resection. Despite its rarity, BSS should be considered in the differential diagnosis when imaging demonstrates a unilateral nasoethmoidal mass that is predominantly isointense to cerebral gray matter on T2-weighted MRI and is hyperostotic on CT.

Key Words: Biphenotypic sinonasal sarcoma, sinonasal malignancy, computed tomography, magnetic resonance imaging, imaging characteristics.

Level of Evidence: 4

INTRODUCTION

Biphenotypic sinonasal sarcoma (BSS), previously referred to as a sinonasal sarcoma with neural and myogenic features, is a recently described tumor of the sinonasal cavity. Histologically, it is characterized as a distinct sinonasal spindle cell neoplasm with uniform, elongated nuclei, and an infiltrative growth pattern.¹ The immunohistochemical profile reveals expression of S100 and actin.^{1,2} The diagnosis is further supported by immunopositivity for B-catenin and immunonegativity for SOX10.^{1,2} It is believed that the dual phenotype of neural and myogenic differentiation stems from recurrent rearrangements in the PAX3 gene, a transcription

factor that promotes differentiation along both lineages.^{2,3} Fluorescence in situ hybridization (FISH) studies reveals numerous rearrangements in the PAX3 gene in BSS.² Despite the consistent and reproducible histologic, cytogenic, and immunophenotypic findings of this tumor, there is limited investigation into the clinical outcomes and imaging characteristics of BSS. While pathology is required for definitive diagnosis, imaging findings may help focus pathologic analysis, elucidate any necessary additional workup, and guide management. In this study, we describe the computed tomography (CT) findings, magnetic resonance imaging (MRI) features, and clinical outcomes of five patients with BSS.

This is an open access article under the terms of the Creative Commons Attribution-NonCommercial-NoDerivs License, which permits use and distribution in any medium, provided the original work is properly cited, the use is non-commercial and no modifications or adaptations are made.

From the Department of Otolaryngology-Head & Neck Surgery (A.M., D.L.), Mayo Clinic, Phoenix, Arizona, U.S.A.; Department of Radiology (S.M.W.), Mayo Clinic, Jacksonville, Florida, U.S.A.; Department of Radiology (C.P.W.), Mayo Clinic, Rochester, Minnesota, U.S.A.; Department of Radiology (J.M.H.), Mayo Clinic, Phoenix, Arizona, U.S.A.

Presented at National Skull Base Society 29th Annual Meeting, February 15–17, 2019, Orlando, Florida, USA.

This study was approved by the Mayo Clinic Institutional Review Board.

Financial Disclosures and Conflict of Interest: None.

Send correspondence to Amar Miglani, MD, Department of Otorhinolaryngology-Head and Neck Surgery, 5777 E. Mayo Boulevard, Phoenix, AZ 85054. E-mail: miglani.amar@mayo.edu

DOI: 10.1002/liv.2.305

tumor recurrence, and survival. Local recurrences were defined as pathologically proven BSS recurring in the sinonasal region. Regional recurrences were defined as BSS recurring in the cervical lymph nodes, while all other locations were defined as distant metastases.

MRI and CT images were reviewed by a board-certified neuroradiologist with 11 years of post-fellowship experience in head and neck radiology. In addition to documenting the tumor epicenter, laterality, and three-dimensional size, involvement of the nasal cavity, nasal septum, adjacent paranasal sinuses, orbit, and anterior skull base was specifically reviewed. The CT images were used to assess tumor-related bone erosion, sclerosis and hyperostosis, while tumor enhancement pattern and T1/T2 signal characteristics were evaluated with MRI.

RESULTS

Five patients with preoperative imaging available for review (Table I) underwent surgical resection of BSS. The median patient age was 56 years (range, 44–69) and 80% ($n = 4$) were female. Negative margins were achieved in four (80%) patients. One patient underwent a gross total resection with microscopic positive margins involving the medial rectus muscle. This patient was advised to undergo radiation therapy following resection. Median post-operative follow-up for this cohort was 31.4 months (range, 2–97 months). Two (40%) patients developed local tumor recurrences (3 and 39 months following treatment). One patient who recurred underwent salvage resection with adjuvant radiation therapy using proton beam. There were no regional or distant tumor metastases, or deaths within the patient follow-up review period.

Three out of five cases underwent open resection with a bifrontal craniotomy for removal of tumor. Two of the cases underwent endoscopic resection. In one case of skull base erosion, dura was resected and sampled and was found to be negative for malignancy. In two cases where lamina was eroded, periorbita was resected—in one patient the periorbita was not involved and in another

TABLE I.
Patient Characteristics and Clinical Outcomes.

| Characteristic | BSS ($n = 5$) |
|---------------------------------|------------------------------|
| Sex | |
| Male | 1 (20%) |
| Female | 4 (80%) |
| Median age (range) | 56 years (44–69 years) |
| Median follow-up (range) | 31.4 months (2–97 months) |
| Negative surgical margins | 4 (80%) |
| Adjuvant radiation | 1 (20%) |
| Local recurrence | 2 (40%) |
| Median time to local recurrence | 20.9 months |
| Regional recurrence | 0 (0%) |
| Distance failure | 0 (0%) |

TABLE II.
Imaging characteristics.

| Characteristic | BSS |
|---|----------|
| Median size ($n = 5$) | |
| Antero-posterior (cm) | 3.4 cm |
| Transverse (cm) | 2.8 cm |
| Craniocaudal (cm) | 3.8 cm |
| Epicenter/origin ($n = 5$) | |
| Ethmoid and nasal cavity | 5 (100%) |
| Laterality ($n = 5$) | |
| Right | 4 (80%) |
| Left | 1 (20%) |
| Bilateral | 0 (0%) |
| Nasal septum involvement ($n = 5$) | |
| No contact | 0 (0%) |
| Contact without erosion | 4 (80%) |
| Contact with erosion | 1 (20%) |
| Sinonasal involvement ($n = 5$) | |
| Ethmoid | 5 (100%) |
| Maxillary | 3 (60%) |
| Sphenoid | 2 (40%) |
| Frontal | 3 (60%) |
| Nasal cavity | 5 (100%) |
| Orbital involvement ($n = 5$) | |
| No involvement | 0 (0%) |
| Contact of lamina papyracea without erosion | 3 (60%) |
| Contact of lamina papyracea with erosion | 2 (40%) |
| Anterior skull base involvement ($n = 5$) | |
| No involvement | 0 (0%) |
| Contact without erosion | 3 (60%) |
| Contact with erosion | 2 (40%) |
| Hyperostosis ($n = 5$) | |
| Present | 4 (80%) |
| Absent | 1 (20%) |
| T1-weighted MRI signal ($n = 4$)* | |
| Isointense | 2 (50%) |
| Background isointense with foci of hypointensity | 2 (50%) |
| T2-weighted MRI signal ($n = 4$)* | |
| Isointense | 1 (25%) |
| Background isointense with foci of hypointensity | 2 (50%) |
| Background isointense with foci of hypointensity and hyperintensity | 1 (25%) |
| MRI enhancement pattern ($n = 4$) | |
| No enhancement | 0 (0%) |
| Homogenous enhancement | 1 (25%) |
| Heterogenous enhancement | 3 (75%) |

*MRI signal characteristics are compared relative to cerebral gray matter.

there was involvement of the periorbita and medial rectus. In the patient with involvement of the medial rectus, radiation treatment was advised but the patient refused treatment and is clinically without evidence of progressive disease at this time.

In references to the two patients with recurrent disease, both recurrences were unifocal and treated with

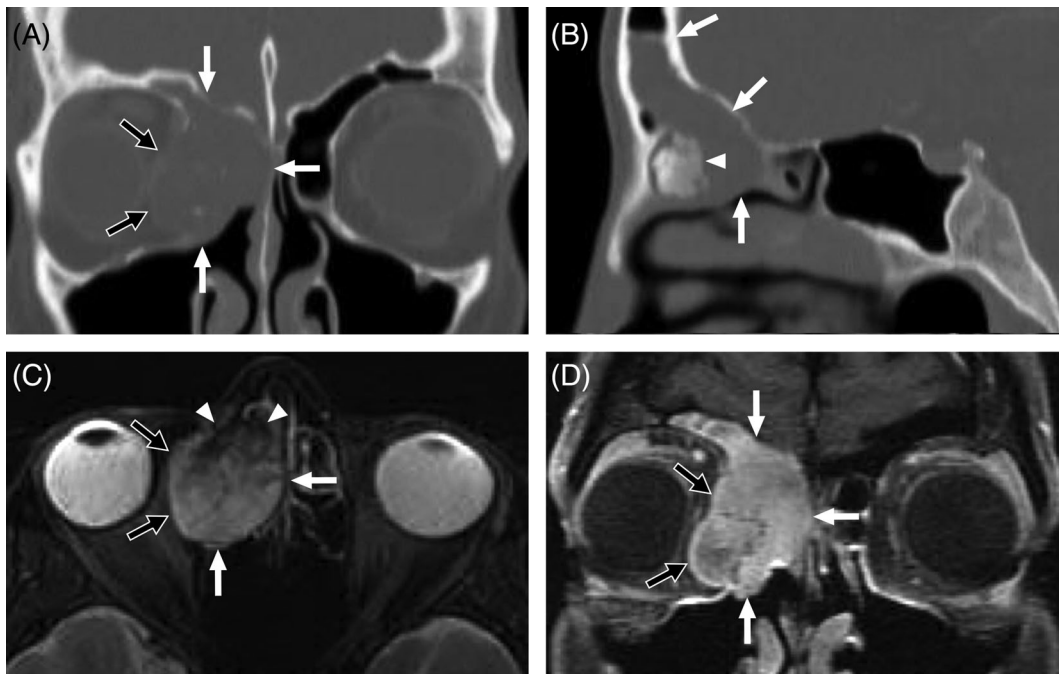


Fig. 1. Imaging features of BSS in a 58 year-old woman. (A) Coronal contrast-enhanced CT. (B) Sagittal contrast-enhanced CT. (C) Axial T2-weighted MRI with fat saturation. (D) Coronal contrast-enhanced T1-weighted MRI with fat saturation. A large heterogeneously enhancing mass (white arrows) centered in the right anterior ethmoid air cells and upper nasal cavity extends from the medial right orbit to the nasal septum and also protrudes superiorly through the right frontal recess. The mass has eroded the right lamina papyracea and invades into the orbit (black arrows) but is still contained by periorbita. A conglomerate area of hyperostosis in present just posterior to the ager nasi (white arrowheads). In addition to T2 hypointensity related to this hyperostosis, the remainder of the mass more posteriorly is heterogeneous on T2-weighted MRI demonstrating mixed isointensity and hyperintensity relative to cerebral gray matter. The anterior skull base is intact, and no intracranial extension is present.

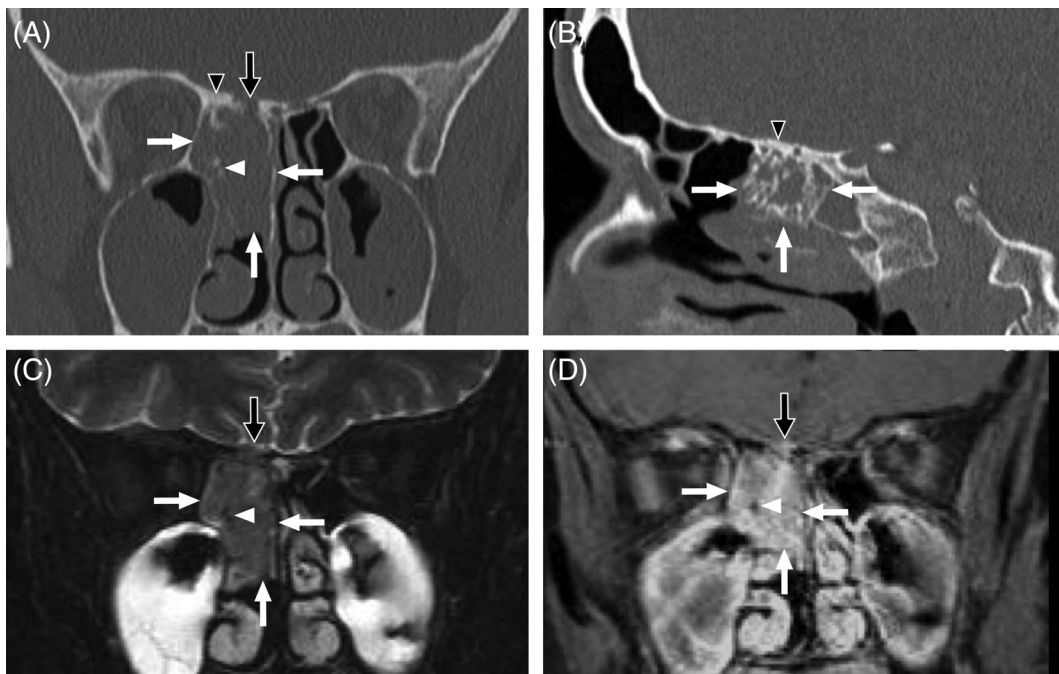


Fig. 2. Imaging features of BSS in a 44 year-old woman. (A) Coronal noncontrast CT. (B) Sagittal noncontrast CT. (C) Coronal T2-weighted MRI with fat saturation. (D) Coronal contrast-enhanced T1-weighted MRI with fat saturation. A sizable tumor (white arrows) occupies the posterior right ethmoidal region and upper nasal cavity extending from nasal septum to right lamina papyracea. Although no orbital invasion is present, the anterior skull base, which is thickened secondary to hyperostosis (black arrowheads), demonstrates focal erosion (black arrows) with a small volume of extra-axial tumor invading the floor of the anterior cranial fossa. The tumor exhibits T2 signal characteristics that are similar to gray matter. The interspersed foci of hyperostosis appear dark on MRI pulse sequences (white arrowheads), which contributes to a pattern of heterogeneous enhancement.

repeat surgical resection. One patient received adjuvant proton beam radiotherapy and did not recur subsequent to treatment. In our series, no adjuvant therapy was used for primary disease. The second patient who recurred underwent a repeat open resection with negative margins. Unfortunately, the patient recurred once more and had a subsequent operation 4 years later again with negative margins. Currently, they are without evidence of disease.

Imaging features of BSS are summarized in Table II. CT was evaluated in the entire cohort, while gadolinium contrast-enhanced MRI was available in four of the five patients. Median tumor size was 3.8 cm (range, 2.7–6.4 cm) in greatest dimension. In all cases, the tumors were unilateral and centered in the nasal cavity and ethmoid sinus. There was a variable degree of involvement of the adjacent sinuses. In all five cases, the tumors extended to the nasal septum, lamina papyracea, and anterior skull base with variable degrees of erosion through these structures. Bony involvement on CT demonstrated a mixed sclerotic and lytic appearance, with definitive hyperostotic bone identified in 80% ($n = 4$) of cases. On MRI, the tumors demonstrated an overall background of T1 and T2 isointensity compared with cerebral gray matter with smaller superimposed foci of dark MRI signal that mostly corresponded to hyperostosis. In one case, the BSS also exhibited interspersed areas of T2 hyperintensity. All cases demonstrated gadolinium enhancement within the tumor and, in 75% of cases, this enhancement was heterogeneous. Figures 1 and 2 illustrate relevant imaging features from two of the patients.

In work-up for metastatic disease, one patient underwent a PET/CT and this revealed no evidence of regional or distant disease. Locally, the tumor was not PET avid, but mucosal thickening was detected. Two patients had CT imaging of the chest, abdomen, and pelvis and these did not reveal any distant disease. In reference to imaging characteristics of recurrent disease, both patients had unifocal localizing areas of recurrences measuring approximately 1.5 cm in greatest dimension.

DISCUSSION

BSS is a rare sinonasal malignancy with very few reported cases in the literature.^{1,4} The emphasis of this study was on the imaging characteristics and clinical outcomes of this rare type of sinonasal neoplasm. This paper describes the outcomes and CT/MRI imaging characteristics of five patients with BSS treated at a large academic health care system. The diagnosis of BSS is made by identifying characteristic histology and immunopositivity for S100 and actin, which was noted in all five patients within our cohort. Further testing with B-catenin and SOX100 can aid in accurately diagnosing this tumor.² FISH studies can also assist in the diagnosis by revealing numerous rearrangements in the PAX3 gene. In comparison to other sinonasal malignancies, such as sinonasal mucosal melanoma with 5-year survival rates on the order of 30%–40%,⁵ BSS has a relatively more favorable prognosis. In our cohort, no patients succumbed to the disease at a median follow-up of 31.4 months. However, there was a high rate of local recurrence (40%) consistent with the previously published case series.^{1,4} Both patients who recurred underwent

salvage surgery and one patient underwent adjuvant radiation following resection. They are currently without evidence of disease at this time.

Cannon et al reviewed rates of recurrences at their institution and of the previously published 29 cases in the literature.⁴ Of the 29 cases, the recurrence rate was noted to be 41% with a 7.8 year follow-up. In reviewing the characteristics of this cohort, there appeared to be less aggressive disease with a smaller portion of patients exhibiting skull base (21%) and/or orbital involvement (24%) in comparison to our series, which demonstrated 100% involvement of the orbit and skull base.⁴ In Cannon's cohort of three patients, there was similarly aggressive disease with 100% of patients exhibiting skull base and/or orbital involvement. Follow-up was only available for two patients and one patient (50%) recurred with a median follow-up of 2.1 years. The recurrence rate for our cohort of five patients was 40% with a median follow-up of 2.6 years. Although our results are consistent with prior studies, the variability noted may be related to tumor stage at presentation. Additionally, adjuvant radiotherapy was not utilized in the vast majority of cases. Given the high rate of local recurrence, consideration of adjuvant radiotherapy may be a reasonable management strategy, but further studies investigating the efficacy and need for radiation treatment are warranted.

CT and MRI studies are often complementary in the information they provide regarding sinonasal neoplasms. CT provides superior bony detail such as erosion of the lamina papyracea, nasal septum or anterior skull base, and also effectively characterizes hyperostosis. MRI is ideal for characterizing the soft tissue component of masses and defining margins relative to post-obstructive, retained secretions. While these imaging studies effectively depict sinonasal abnormalities, there is considerable overlap in the imaging appearance of sinonasal tumors.⁶ Nevertheless, the current observations combined with previously published cases^{1,4} suggest that certain imaging features, although not entirely specific to BSS, at least warrant inclusion of BSS in the differential diagnosis.

From an imaging standpoint, the epicenter for all five patients involved the nasal cavity and ethmoid sinus, and all presented as unilateral masses. The average greatest dimension of the tumor was 3.8 cm suggesting that these patients present with a moderate amount of tumor bulk. This is further supported by the findings that all cases demonstrated involvement of the septum, skull base, and lamina papyracea at the time of diagnosis. Hyperostosis was a common finding (80%) and was also present in all three of the cases previously described by Cannon et al.⁴ However, hyperostosis is not a finding that is unique to BSS, as it can be noted in other tumor types and disease processes such as meningiomas, benign nasal tumors, other sinonasal malignancies, and inflammatory disease.^{7–9}

On MRI, the noncontrast T1-weighted imaging features and enhancement pattern of BSS are quite non-specific. However, BSS demonstrates mainly T2 signal that is similar to cerebral gray matter and lower than that of many other sinonasal neoplasms. This is common in fibrotic and highly cellular tumors and, indeed, BSS has been characterized as a spindle cell neoplasm with

cellularity that is quite high.¹ Superimposed foci of very dark MRI signal may be identified in relation to areas of hyperostosis. Interestingly, one BSS also exhibited heterogeneous areas of T2 hyperintensity. Since it is not possible to retrospectively correlate the imaging with the resected tumor in a stereotactic fashion, the significance of this is unclear. However, a subset of BSS exhibits a pattern of epithelial proliferation with invaginations of cystic spaces or small glands beneath the mucosal surface.¹ Perhaps this admixture of glandular structures with neoplastic spindle cells may have contributed to the more heterogeneous T2 signal characteristics in this one case.

CONCLUSION

BSS is a locally aggressive tumor, with low risk of regional or distant metastases but has a significant rate of recurrence even in the setting of adequate resection. In spite of its rarity, BSS should be included in the differential diagnosis when imaging demonstrates a unilateral nasoethmoidal mass that is predominantly isointense to cerebral gray matter on T2-weighted MRI and exhibits hyperostosis on CT.

BIBLIOGRAPHY

1. Lewis JT, Oliveira AM, Nascimento AG, et al. Low-grade sinonasal sarcoma with neural and myogenic features: a clinicopathologic analysis of 28 cases. *Am J Surg Pathol* 2012;36(4):517–525.
2. Rooper LM, Huang S, Antonescu CR, Westra WH, Bishop JA. Biphenotypic sinonasal sarcoma: an expanded immunoprofile including consistent nuclear β -catenin positivity and absence of SOX10 expression. *Hum Pathol* 2016;55:44–50. <https://doi.org/10.1016/j.humpath.2016.04.009>.
3. Wang X, Bledsoe KL, Graham RP, et al. Recurrent PAX3-MAML3 fusion in biphenotypic sinonasal sarcoma. *Nat Genet* 2014;46(7):666–668. <https://doi.org/10.1038/ng.2989>.
4. Cannon RB, Hunt JP, Iii RHW, Witt BL. Imaging and outcomes for a new entity: low-grade sinonasal sarcoma with neural and myogenic features. *J Neurol Surg Rep* 2017;78(1):15–19.
5. Miglani A, Patel SH, Kosiorek HE, Hinni ML, Hayden RE, Lal D. Endoscopic resection of sinonasal mucosal melanoma has comparable outcomes to open approaches. *Am J Rhinol Allergy* 2017;31(3):200–204. <http://www.ingentaconnect.com/content/ocean/ajra/2017/00000031/00000003/art00012>.
6. Koeller KK. Radiologic features of sinonasal tumors. *Head Neck Pathol* 2016; 10(1):1–12. <https://doi.org/10.1007/s12105-016-0686-9>.
7. Lee DK, Chung SK, Dhong H, Kim H, Bok KH. Focal hyperostosis on CT of sinonasal inverted papilloma as a predictor of tumor origin. *Am J Neuroradiol* 2007;28(4):618–621.
8. Chiu AG, Jackman AH, Antunes MB, Feldman MD, Palmer JN. Radiographic and histologic analysis of the bone underlying inverted papillomas. *Laryngoscope* 2006;116:1617–1620. <https://doi.org/10.1097/01.mlg.0000230401.88711.e6>.
9. Pieper D, Al-Mefty O, Handa Y, Buechner D. Hyperostosis associated with meningioma of the cranial base: secondary changes or tumor invasion. *Neurosurgery* 1999;44(4):742–746.